Photon echo measurements in liquids: Numerical calculations with model systems

Minhaeng Cho and Graham R. Fleming

Citation: The Journal of Chemical Physics **98**, 2848 (1993); doi: 10.1063/1.464114
View online: http://dx.doi.org/10.1063/1.464114
View Table of Contents: http://scitation.aip.org/content/aip/journal/jcp/98/4?ver=pdfcov
Published by the AIP Publishing

Photon echo measurements in liquids: Numerical calculations with model systems

Minhaeng Cho and Graham R. Fleming
Department of Chemistry and the James Franck Institute, The University of Chicago, Chicago, Illinois 60637

(Received 17 August 1992; accepted 28 October 1992)

Two- and three-pulse photon echo signals are calculated for various model systems. The use of an experimental solvation correlation function as the solvent fluctuation correlation function leads to two conclusions. First, inertial solvent motion plays a major role in the electronic dephasing process. Second, simple models such as Markovian or exponential models for the solvent fluctuation correlation function may not provide an adequate description of the echo signal. The real and imaginary parts of the echo response, which may be measured via heterodyne detected stimulated photon echoes, are compared with conventional photon echo signals.

I. INTRODUCTION

The dynamical aspects of the solvent response are critical in understanding a wide range of condensed phase phenomena such as electron transfer,[1] chemical reactions,[2] and spectroscopic line shapes.[3] An important probe of the interaction of solvents and solutes is the absorption spectrum of a chromophore. The absorption spectrum is broadened by various mechanisms, for example, pure dephasing, inhomogeneous broadening, and lifetime broadening. It is often the case that the largest contribution to the spectral width arises from the inhomogeneous distribution of the local environments of the solute molecules. For example, in the case of crystals or glassy materials an impurity chromophore is located in a structured and virtually time-invariant environment. On the other hand, in solution, the local structure of the solvent around the chromophore is, in general, fluctuating, and is not well characterized compared to the solid system. Transitions between different inherent structures take place on a wide range of time scales.[4]

When the chromophore interacts with an external optical field the first interaction produces an electronically coherent state. The electronic phase of this state is determined by the quantity $\omega_{eg}(t)$ representing the time-dependent electronic transition frequency between the electronic ground and excited states. The optical transition frequency of the ith chromophore can be written in the form

$$\omega_{eg}^{i}(t)=\langle\omega_{eg}\rangle+\varepsilon_i+\Delta\omega_i(t) \tag{1}$$

where $\langle\omega_{eg}\rangle$ is the average optical transition frequency for all the chromophores, ε_i represents a static contribution determined by the local environment of the ith chromophore, and $\Delta\omega_i(t)$ is a fluctuating term induced by the dynamical aspects of the surrounding media. Here it is assumed that the time scale associated with changes in ε_i is very long compared with that of $\Delta\omega_i(t)$. Furthermore, it is usually assumed that the fluctuating term is common for all chromophores, thus, $\Delta\omega(t)=\Delta\omega_i(t)$. This assumption justifies the use of the term homogeneous dephasing. The phase of the electronically coherent states created by the interaction with the external field is determined by not only the fluctuations term $\Delta\omega(t)$ around $\langle\omega_{eg}\rangle$ but also by ε_i. Since $\Delta\omega(t)$ is defined as the fluctuating frequency around the average value $\langle\omega_{eg}\rangle$, the average of $\Delta\omega(t)$ is zero. In calculations of the absorption spectrum as well as various nonlinear spectroscopic measurements, the correlation function of the solvent fluctuation $\Delta\omega(t)$ plays a key role. As we shall show later, the mean-square amplitude of the solvent fluctuations $\langle\Delta\omega^2\rangle$ (times a solvent correlation time—see Sec. III) determines the magnitude of the homogeneous contribution to the line broadening. Assuming that the solvent modes are strongly coupled to the electronic excitation of a chromophore, Harris *et al.*[5] developed a simplified model describing the dephasing phenomena. In this model, the mean-square amplitude of the solvent fluctuation can be related to both the displacements and the frequencies of the solvent modes.

One of the critical questions relating to the validity of Eq. (1) is whether a time-scale separation between the inhomogeneous and homogeneous contributions associated with ε_i and $\Delta\omega(t)$, respectively, really exists. Such a time-scale separation clearly exists in the case of crystals or glassy materials. However, it is not clear that this assumption is valid for liquid systems, since a broad distribution of time scales for the molecular motions exists with no clear cut division into two parts. In order to make a comparison between the two time scales, the width of the inhomogeneous distribution of ε should be compared with the average time scale of the dynamical solvent motions. Recently, Shemetulskis and Loring[6] calculated the absorption spectrum for a model system consisting of a dipolar solute in a dipolar solvent based on an inhomogeneous approximation. They found in their simulated system that the inhomogeneous contribution to the line broadening was the dominant mechanism.

As discussed earlier, linear spectroscopic techniques cannot be used to selectively measure the dynamical contributions of the solvent. In order to overcome this difficulty, photon echo measurements have been widely used to obtain information on the dynamical aspects of the solvent

 0021-9606/93/042848-12$06.00

without contamination from the inhomogeneous contribution.[7,8] For a two-pulse photon echo measurement, the first pulse with wave vector $\mathbf{k}_1$, creates an electronically coherent state. The following pulse with wave vector $\mathbf{k}_2$ switches the phase of the coherent state by π with respect to that of the first optical coherent state.[8] Now, the rephasing process creates coherent echo fields produced by the macroscopic third-order material polarizations in the directions $2\mathbf{k}_2-\mathbf{k}_1$ and $\mathbf{k}_1$ with frequencies of $2\omega_2-\omega_1$ and ω_1, respectively, although the echo field whose wave vector $2\mathbf{k}_2-\mathbf{k}_1$ is usually considered to be the photon echo field. During this critical rephasing process, the inhomogeneous contribution is eliminated and the echo field is centered at time $t=t_0$ from the second pulse, where the two pulses are separated by a time t_0. Formally, the electronic phases of the two electronic coherence states of the ith chromophore should be averaged over the ensemble,

$$S_{\text{total}}(\mathbf{k}_s=2\mathbf{k}_2-\mathbf{k}_1;t_0,t) = S_{\text{echo}}(t_0,t)\left|\int d\varepsilon\, f(\varepsilon)\exp[\pm i\varepsilon(t_0-t)]\right|^2, \quad (2a)$$

$$S_{\text{total}}(\mathbf{k}_s=\mathbf{k}_1;t_0,t) = S_{\text{echo}}(t_0,t)\left|\int d\varepsilon\, f(\varepsilon)\exp[\pm i\varepsilon(t_0+t)]\right|^2, \quad (2b)$$

where t denotes the time after the second pulse. Combinations of signs in Eq. (2) are specified by the four Liouville pathways described by Yan and Mukamel.[9] Here $f(\varepsilon)$ represents the distribution of the inhomogeneity factor ε. S_{echo} is the echo signal without the inhomogeneous contribution. When the distribution $f(\varepsilon)$ is broad and t and t_0 have opposite signs as in Eq. (2a), the integration shown above is sharply peaked at $t=t_0$, since both t and t_0 are defined positive. This is the case when the signal from Eq. (2b) disappears. The echo signal is thus observed when the time from the second pulse is equal to the delay time between the two pulses. The decrease of the photon echo signal intensity with respect to t_0 is purely induced by the homogeneous contribution.

The final two interactions with the field are coincident, in the two pulse echo and thus the signal does not contain contributions from the shift in energy of the excited state resulting from solvent relaxation (i.e., the Stokes shift or spectral diffusion). By introducing an additional controllable time interval for the three-pulse photon echo measurement, the dynamical evolution of the population state can also be studied by varying the delay time between the second and third pulses. The wave vector of the three-pulse photon echo field is given as $\mathbf{k}_3+\mathbf{k}_2-\mathbf{k}_1$, when $\mathbf{k}_i$ denotes the wave vector of the ith pulse. When the echo fields are directly measured, the two-pulse and three-pulse stimulated photon echo signals are proportional to the square of the material field.[9] By contrast, the accumulated and heterodyne-detected photon echo signals give the real part and both the real and imaginary parts of the echo field, respectively.[10]

In the case of a small inhomogeneous contribution to the linewidth the rotating wave approximation leads to the generation of two coherent fields with wave vectors $\mathbf{k}_3-\mathbf{k}_2+\mathbf{k}_1$ and $\mathbf{k}_3+\mathbf{k}_2-\mathbf{k}_1$.[11] As the width of the inhomogeneous distribution increases the signal along $\mathbf{k}_3+\mathbf{k}_2-\mathbf{k}_1$ becomes dominant and represents the echo signal.[11(a),11(d)]

Shank and co-workers measured both two-pulse[12] and three-pulse[13] photon echo signals of Nile Blue in various polar liquids. They analyzed the observed signals under the assumption that the solvent fluctuations obey Gaussian dynamics. For fixed delay times between the first and third pulses, the echo signals show the same decay patterns, leading to the interpretation that the homogeneous dephasing constants range from 20 to 80 fs in various polar liquids. These authors found that a truncated exponential for the solvent fluctuation correlation function gave a satisfactory description of their experimental observations. Wiersma and co-workers[14] carried out two-pulse photon echo measurements for resorufin in DMSO solution and used the exponential model (also called the stochastic model or the Kubo line-broadening function) to fit their data. We shall also use an exponential model to numerically calculate the echo signals and discuss the validity and limitations of this model by comparing these results with the echo signals calculated by using the solvent fluctuation correlation function measured by the time-dependent fluorescence Stokes shift technique.

In the present paper, we calculate various photon echo signals numerically, using the cumulant expansion expressions for the nonlinear response function developed by Mukamel and co-workers.[15,16] Our goal is to clarify the role of solvent dynamics in the form of the various types of echo signals. In particular, we wish to investigate the importance of inertial contributions[6(b),17,18] to the solvent dynamics and the connections between echo measurements and other ultrafast studies of solvation such as fluorescence Stokes shift measurements.[19] We also discuss the additional information which can be obtained from echo measurements, particularly when both the real and imaginary parts of the signal are obtained. The theoretical aspects of the nonlinear response functions and echo signals are summarized in Sec. II. Four different model systems of the solvent fluctuation correlation function are discussed (Sec. III). The first model system corresponds to the Markovian limit, in which the solvent correlation time is very short compared with the dynamical time scale of the system. The second model considers an exponential function with a moderate time constant for the solvent fluctuation correlation function. In the third model, we use the experimentally obtained solvation correlation function by Rosenthal *et al.*[18] for the solvent fluctuation correlation function, since this includes various types of the solvent motions with a wide range of timescales. Finally, a Gaussian approximation to the solvation correlation function is used to investigate the role of inertial behavior. We calculate response functions associated with the photon echo signals in Sec. IV and discuss the results in Sec. V.

II. THEORETICAL

The third-order polarization obtained by expanding the density operator up to the third order with respect to

the external field $E(t)$ can be calculated by using eight nonlinear response functions representing the eight Liouville pathways.[16] Mukamel[15] has developed a theoretical description for the response functions using cumulant expansion techniques. Assuming that the solvent fluctuations obey Gaussian statistics makes it possible to truncate the cumulant expansions at the second-order terms.

Femtosecond photon echo signals are described by the nonlinear response functions that control all four-wave mixing spectroscopies.[9,10] Although four contributions and their complex conjugate are necessary to fully describe all four-wave mixing spectroscopies, in the limit of large inhomogeneity two out of four pathways become vanishingly small. These two response functions correspond to the cases where the electronic phase, determined by the inhomogeneity factor ε, is given by $\exp[\pm i\varepsilon(t_1-t)]$ [see Eq. (2)]. In the large inhomogeneous broadening limit, the relevant response functions for the echo generation are given by[9]

$$R_1(t_3,t_2,t_1)=\exp[-g^*(t_3)-g^*(t_1)+g(t_2)-g(t_2+t_3) -g^*(t_1+t_2)+g^*(t_1+t_2+t_3)], \tag{3a}$$

$$R_2(t_3,t_2,t_1)=\exp[-g(t_3)-g^*(t_1)+g^*(t_2)-g^*(t_2+t_3) -g^*(t_1+t_2)+g^*(t_1+t_2+t_3)], \tag{3b}$$

where

$$g(t)=i\lambda\int_0^t d\tau_1 M(\tau_1)+\langle\Delta\omega^2\rangle\int_0^t d\tau_1\int_0^{\tau_1} d\tau_2 M(\tau_2) \tag{4}$$

and

$$M(t)=\frac{\langle\Delta\omega(0)\Delta\omega(t)\rangle}{\langle\Delta\omega^2\rangle}. \tag{5}$$

To obtain the above expressions, classical approximations were introduced to the time-ordered exponential and energy gap operator by replacing the usual exponential function and time-dependent energy gap (not an operator), respectively.[15]

We define σ as the zero-frequency Laplace transform of $M(t)$:

$$\sigma\equiv\int_0^\infty dt M(t). \tag{6}$$

The line-shape function $g(t)$ carries all the dynamical information determining both spectral diffusion and decay of the photon echo signals. These two contributions correspond to the first and second terms in Eq. (4), respectively. λ is the magnitude of the energy shift of the excited state resulting from the solvation process (Stokes shift). The decay of the correlation function $M(t)$ directly influences the time-dependent properties of the nonlinear response functions. Here, it is assumed that the solvent fluctuations obey Gaussian statistics so that the second-order cumulant expansion is exact.

For simplicity, we define the response function $R(t_3,t_2,t_1)$ as

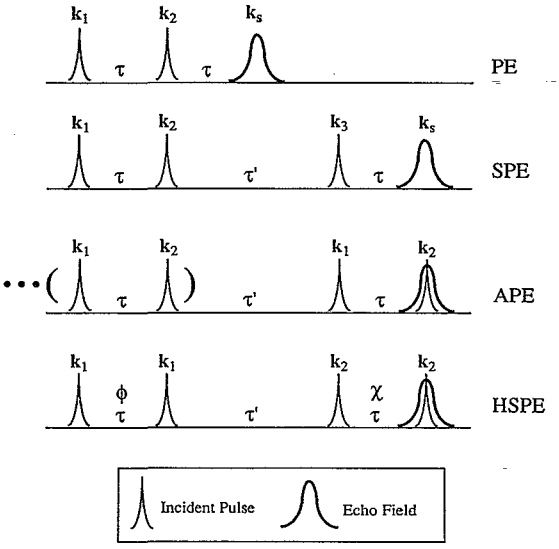

FIG. 1. Pulse sequences for the various photon echo techniques. PE, two-pulse photon echo; SPE, stimulated photon echo; APE, accumulated photon echo; HSPE, heterodyne-detected stimulated photon echo. τ is the delay time between the first and second pulses which is roughly equal to the electronic coherence duration time. ϕ and χ are optical phases between the first and second pulses and between the third and the local oscillator fields, respectively; $\psi=\phi-\chi$.

$$R(t_3,t_2,t_1)=R_1(t_3,t_2,t_1)+R_2(t_3,t_2,t_1). \tag{7}$$

Given the response functions calculated from $M(t)$, we can summarize the various types of photon echo signals as functions of $R(t_3,t_2,t_1)$:

$$S_{\rm PE}(\tau)=|R(\tau,0,\tau)|^2, \tag{8a}$$

$$S_{\rm SPE}(\tau,\tau')=|R(\tau,\tau',\tau)|^2, \tag{8b}$$

$$S_{\rm HSPE}(\tau,\tau',\psi=0)=S_{\rm APE}(\tau,\tau')={\rm Re}[R(\tau,\tau',\tau)], \tag{8c}$$

$$S_{\rm HSPE}(\tau,\tau',\psi=\pi/2)=-{\rm Im}[R(\tau,\tau',\tau)], \tag{8d}$$

where PE, SPE, APE, and HSPE denote photon echo, stimulated photon echo, accumulated photon echo, and heterodyne-detected stimulated photon echo, respectively.[10] Detailed theoretical descriptions of these photon echoes were given in Refs. 9 and 10. Pulse sequences and delay times between pulses are indicated in Fig. 1. The phase difference ψ $(=\phi-\chi)$ in the heterodyne-detected stimulated photon echo (HSPE) experiments is the optical phase difference between the third pulse and the local oscillator fields. τ and τ' are the duration periods of the electronic coherence states and the population states, respectively. Measuring a τ-dependent decay of the echo signals provides information on the optical dephasing process induced by the dynamical fluctuations of the solvent. On the other hand, a τ'-dependent measurement can be used to understand the solvation dynamics, as demonstrated by the numerical calculations of Bosma *et al.*[20] Vibrational quantum beats can also be observed in the τ'-dependent signal, since the second-order interaction with the chromophore creates vibrational coherences in both the ground and excited states. Since vibrational dephasing processes

can be studied by other spectroscopic techniques, in this paper we focus on the role of the solvent in the optical dephasing process.

III. MODEL SYSTEMS

As seen in Eq. (4), knowledge of $M(t)$, the magnitude of the Stokes shift, and the magnitude of the solvent fluctuations is sufficient to calculate the various echo signals. In case of the Markovian limit, the correlation function $M(t)$ is a δ function, $M(t)=\sigma^{-1}\delta(t)$. In this limit the line-shape function $g(t)$ is

$$g_B(t)=i\frac{\lambda}{\sigma}+\frac{\langle\Delta\omega^2\rangle}{\sigma}t. \tag{9}$$

This is a *Bloch* approximation, wherein the inverse of the dephasing constant determining the homogeneous width of the Lorentzian absorption and fluorescence spectra is given by $\langle\Delta\omega^2\rangle/\sigma$.

The second model we use is an exponential model for $M(t)$, $M(t)=\exp(-t/\tau_c)$. The solvent nuclear relaxation is characterized by a correlation time τ_c. The corresponding $g(t)$ is then

$$g_E(t)=i\lambda\tau_c[1-\exp(-t/\tau_c)] + \langle\Delta\omega^2\rangle\tau_c^2[\exp(-t/\tau_c)+t/\tau_c-1], \tag{10a}$$

where subscript "E" denotes an *exponential* correlation function. The exponential model has been used to simulate an overdamped solvation correlation function.[14,20] If no spectral diffusion is assumed, the well-known Kubo line-shape function[21] is obtained. In the long time limit ($\tau\gg\tau_c$), the line-shape function approaches an asymptotic limit,

$$g_E(t\gg\tau_c)=i\lambda\tau_c+\langle\Delta\omega^2\rangle\tau_c t=i\frac{\lambda}{\sigma}+\frac{\langle\Delta\omega^2\rangle}{\sigma}t. \tag{10b}$$

This limiting behavior can also be observed when the correlation time constant τ_c approaches zero. The second equality is obtained from the fact that the zero-frequency Laplace transform of the exponential model shows that σ is equal to τ_c^{-1}. The long-time behavior of the exponential model approaches the Markovian description as expected [compare Eqs. (9) and (10b)]. Thus the decay pattern in this asympotic limit is identical to that of the Markovian limit.

We now turn to the next model system. The time-dependent fluorescence Stokes shift (TDFSS) correlation function is defined by

$$S(t)=\frac{\nu(t)-\nu(\infty)}{\nu(0)-\nu(\infty)}, \tag{11}$$

where $\nu(0)$, $\nu(\infty)$, and $\nu(t)$ are the initial, final, and time-dependent fluorescence frequencies. In the linear-response approximation, the time-dependent Stokes shift is equal to the normalized autocorrelation function of the fluctuations in solvation energy difference $\Delta\omega(t)$,

$$S(t)=C(t)=\frac{\langle\Delta\omega(0)\Delta\omega(t)\rangle}{\langle\Delta\omega^2\rangle}, \tag{12}$$

where $\Delta\omega(t)$ is propagating on the ground-state potential-energy surface. The angular bracket denotes an average over the equilibrium nuclear degrees of freedom in the ground state. The third model we have used for $M(t)$ is the experimentally determined $S(t)$ obtained by Rosenthal *et al.*[18] for the dye LDS-750 dissolved in acetonitrile. The correlation function obtained by Rosenthal *et al.* contains features we expect to be quite general. The decay includes both inertial behavior of the solvent molecules and slower components resulting from the collective motions. It should be noted that to calculate the echo signals we assume (i) a linear-response approximation for the solvation dynamics and that (ii) $\Delta\omega(t)$ is propagating on the ground state. Several molecular-dynamics simulations have addressed the reliability of the linear response approximation. It appears to be quite good in most cases.[17,22–24] For large polyatomic solute molecules, this approximation is expected to be good.[18] As for the second approximation, Shemetulskis and Loring[6(b)] carried out molecular-dynamics simulation studies with a semiclassical expression for the two-pulse photon echo signal, in which the effective Hamiltonian is given by the arithmetic average of the ground and excited state Hamiltonians. They found that the discrepancy between echo signals calculated by using both the effective and ground state Hamiltonians was very small. This observation suggests that both the amplitude of the solvent fluctuations and the solvent fluctuation correlation function are not sensitive functions of the electric properties of the solute molecule. Fried *et al.*[25] also calculated response functions by using several Brownian oscillators to represent the solvation correlation function, where the ensemble average was taken over the ground state nuclear degrees of freedom. Replacing $M(t)$ with $S(t)$, we obtain the line-shape function $g(t)$:

$$g_S(t)=i\lambda\int_0^t d\tau_1 S(\tau_1)+\langle\Delta\omega^2\rangle\int_0^t d\tau_1\int_0^{\tau_1}d\tau_2 S(\tau_2). \tag{13}$$

Because of the complexity of $S(t)$, the line-shape function cannot be written analytically in this case.

Molecular-dynamics simulation studies of acetonitrile[22(b)] and CH_3Cl,[17] and recent Stokes shift experiments[18] on acetonitrile solution, have shown that the initial decay is governed by the inertial behavior of the solvent molecules. The inertial portion of the decay can be well approximated by a Gaussian function,[17–19] which can be obtained by a short-time expansion of the correlation function $M(t)$. As a final approximation we used a Gaussian function obtained from fitting $S(t)$. Thus, $M(t)=\exp(-t^2/\tau_g^2)$ and

$$g_G(t)=i\lambda\int_0^t d\tau_1\exp(-\tau_1^2/\tau_g^2) + \langle\Delta\omega^2\rangle\int_0^t d\tau_1\int_0^{\tau_1}d\tau_2\exp(-\tau_2^2/\tau_g^2). \tag{14}$$

The time at half height, i.e., $M(t)=\frac{1}{2}$, is $\tau_g\sqrt{\ln 2}$.

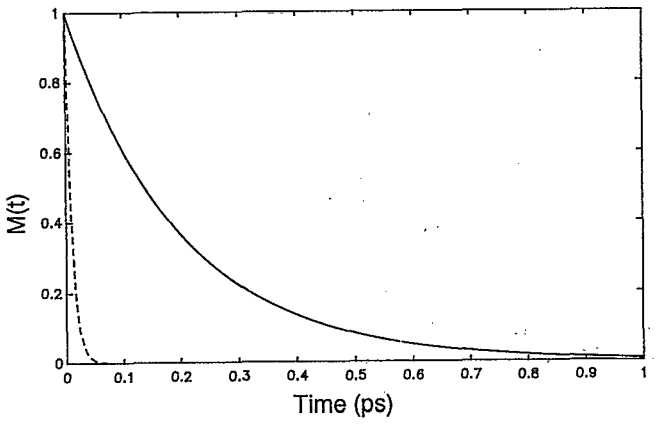

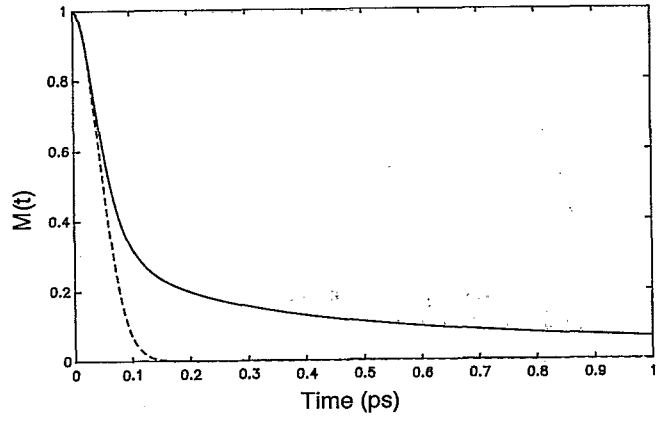

FIG. 2. Model solvent fluctuation correlation functions defined in Eq. (3). (a) Two exponential models whose time correlation functions are 200 (solid line) and 10 fs (dashed line). (b) Solvation correlation function measured experimentally for LDS-750 in acetonitrile (Ref. 19). The dashed curve is a Gaussian fit with τ_g=62 fs.

IV. NUMERICAL CALCULATIONS AND DISCUSSION

In this section, we present echo signals calculated with the various model systems discussed in Sec. III. The parameters are chosen to represent polar liquids. In all calculations (except those in Sec. IV E) we use a value for the mean square of the solvent fluctuation $\langle\Delta\omega^2\rangle$ of 600 ps^{-2}, and ignore contributions from intramolecular vibrational coherences which would be observed as quantum beats in the echo signals.[12] As would be expected from the discussion in Sec. II, the decay of the echo is strongly dependent on the magnitude of the mean square of the fluctuations $\langle\Delta\omega^2\rangle$. It will also become evident that the echo decay is strongly dependent on the decay characteristics of $M(t)$. Although the mean-square amplitude of the solvent fluctuation is related to the magnitude of the Stokes shift, λ, through the fluctuation-dissipation theorem,[9] we consider the two quantities as independent parameters in Sec. IV. E.

In Figs. 2(a) and 2(b), the model $M(t)$'s are shown. The dashed and solid curves in Fig. 2(a) are exponential *functions* whose decay time constants τ_c are 10 and 200 fs, respectively. Thus, the former can be assumed to correspond to the Markovian limit (Bloch approximation) while latter is the case when $M(t)$ is decaying exponentially. The experimentally measured solvation correlation function $S(t)$ of LDS-750 in acetonitrile is drawn in Fig. 2(b) as a solid line. The Gaussian fit to the initial decay of $S(t)$ is shown as the dashed curve in the same figure. It has a decay constant τ_g of 62 fs, that is to say, the standard deviation for this Gaussian $M(t)$ is 44 fs.

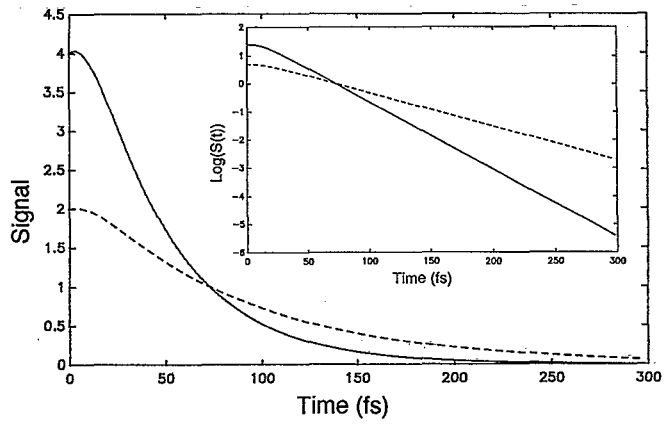

FIG. 3. Echo signal in the Markovian limit. The two-pulse echo signal is calculated using the exponential model with a correlation time of 10 fs. Two-pulse echo signal (solid curve) and real part of the response function (dashed curve) with respect to τ. Inset: logarithmic plots of the same functions with respect to τ.

A. Markovian limit (Bloch approximation) with no spectral diffusion

When the decay time constant of $M(t)$ is 10 fs, we may assume that the fluctuations are in the Markovian limit (impact limit) as the time scale of the system is long compared to 10 fs (fast modulation limit). The dashed curve in Fig. 3 corresponds to the response function $R_B(\tau,\tau'=0,\tau)$. The two-pulse photon echo signal $|R_B(\tau,\tau'=0,\tau)|^2$ is shown as the solid line in Fig. 3. When $\tau'=0$, from Eqs. (8a) and (9),

$$R_B(\tau,\tau'=0,\tau)=2\exp(-2\Gamma\tau)$$

and

$$|R_B(\tau,\tau'=0,\tau)|^2=4\exp(-4\Gamma\tau) \tag{15}$$

with

$$\Gamma=\langle\Delta\omega^2\rangle\tau_c.$$

In our model system, Γ=6 ps^{-1} (Γ^{-1}=167 fs). In the Markovian limit, there is no τ' dependence of R_1 and R_2, and also $R_1=R_2$. Since we assume no spectral diffusion, i.e., $\lambda=0$, the imaginary part of the response function is zero. From the experimental signal, we can obtain the decay rate constant Γ by plotting $\log[|R_B(\tau,\tau'=0,\tau)|^2]$ or $\log[R_B(\tau,\tau'=0,\tau)]$ with respect to τ [see the inset in Fig. 3].

B. Exponential $M(t)$ with no spectral diffusion (Kubo model, Stochastic model, overdamped Brownian oscillator model, Ornstein–Uhlenbeck process)

This is the case when the correlation function is decaying exponentially with modest decay constant (intermediate modulation limit). In our model, the decay time constant τ_c is 200 fs. $R_E(\tau,\tau'=0,\tau)$ and $|R_E(\tau,\tau'=0,\tau)|^2$, and $\log[R_E(\tau,\tau'=0,\tau)]$ and $\log[|R_E(\tau,\tau'=0,\tau)|^2]$ are shown in Figs. 4(a) and its inset, respectively. As can be seen in Fig. 4(b), the echo signal is clearly nonexponential over 300 fs. In this case it is unlikely that the asymptotic exponential behavior of the echo signal would be observable. The two response functions R_1 and R_2 are indentical, but a τ' dependence is manifest as shown in Fig. 4(b). For τ's fixed at 0, 100, and 200 fs, $|R_E(\tau,\tau',\tau)|^2$ is calculated to see the decay of the three-pulse echo signal with respect to τ'.

C. Using the solvation correlation function $S(t)$ for $M(t)$ without Stokes shift (zero λ)

Using the solvation correlation function measured experimentally (see Sec. III), we calculated $|R_S(\tau,\tau',\tau)|^2$.

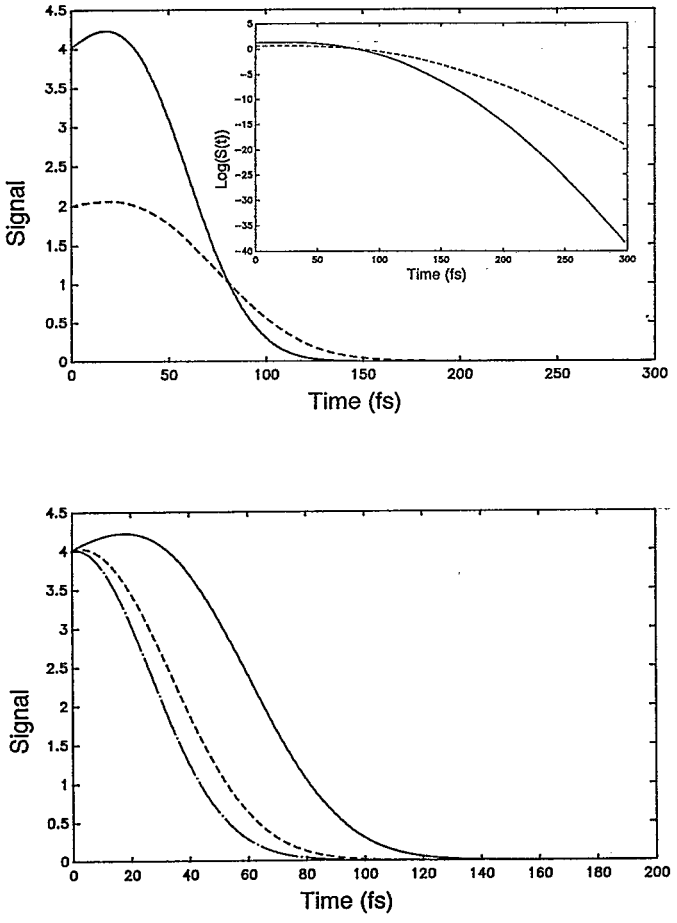

FIG. 4. Exponential model calculation with τ_c=200 fs. (a) The two-pulse echo signal with respect to τ and the real part of the response function are shown as solid and dashed curves, respectively. Inset: logarithmic plots of the same functions. (b) Three-pulse photon echo signals for τ'=0 (solid curve), 100 (dashed curve), and 200 fs (dashed-dotted curve).

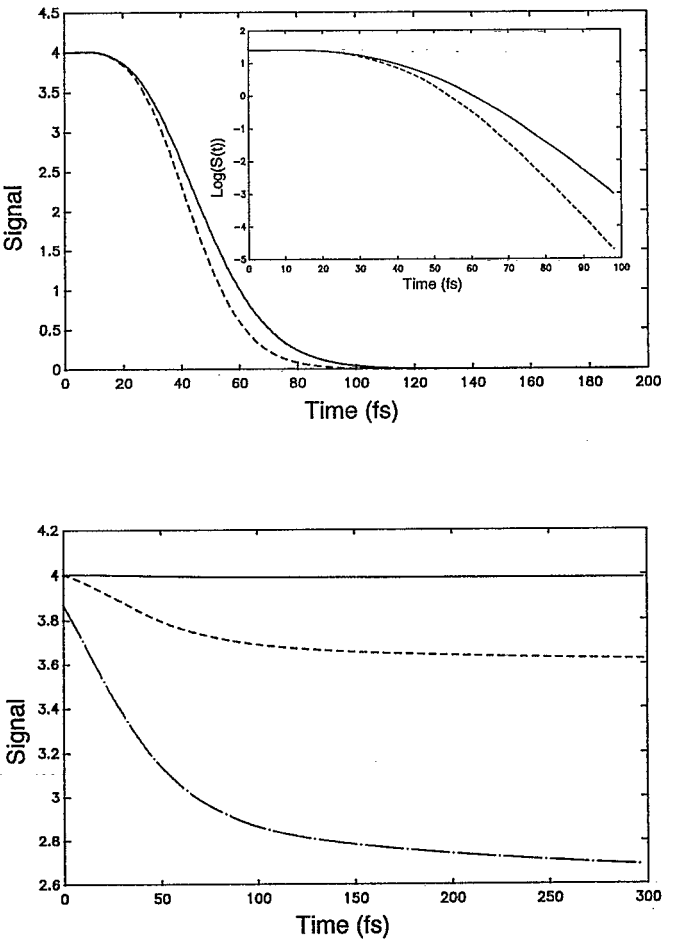

FIG. 5. Signals calculated with both $M(t)=S(t)$ [shown as solid curves in (a)] and a Gaussian approximation to $M(t)$ (dashed curves). (a) Two-pulse photon echo signals. Inset: logarithmic plots of the same functions. (b) Three-pulse photon echo signals with respect to τ' for τ=2 (solid curve), 10 (dashed curve), and 20 fs (dashed-dotted curve).

The Gaussian approximation for $M(t)$ shown in Fig. 2(b) was also used in calculating $|R_G(\tau,\tau',\tau)|^2$. For a two-pulse photon echo, we compare $|R_S(\tau,\tau'=0,\tau)|^2$ and $|R_G(\tau,\tau'=0,\tau)|^2$ in Fig. 5(a). The echo signal with a Gaussian approximation to $M(t)$ is qualitatively very similar to the exact case, but decays more rapidly than $|R_S(\tau,\tau'=0,,\tau)|^2$. The flat region up to 30 fs results from the inertial behavior of the solvent molecules. The difference between the Gaussian approximation and the exact calculation is obvious in the logarithmic plots of the inset in Fig. 5(a). Nonexponential behavior is also clear in both the exact and Gaussian approximation two-pulse echo signals. The difference in the two signals results mainly from the small deviation of the Gaussian curve and $S(t)$ within the first 100 fs [see Fig. 2(b)].

Three-pulse echo signals with respect to τ' are shown in Fig. 5(b) for τ=2, 10, and 20 fs. For small values of τ, the change of the τ'-dependent signal is small. This can be understood by putting a small number for t_1 and t_3 in Eqs. (3a) and (3b). If τ becomes very large, the change is also small because $g(t=\infty)=0$. The decays in Fig. 5(b) all clearly show bimodal character, but this does not include

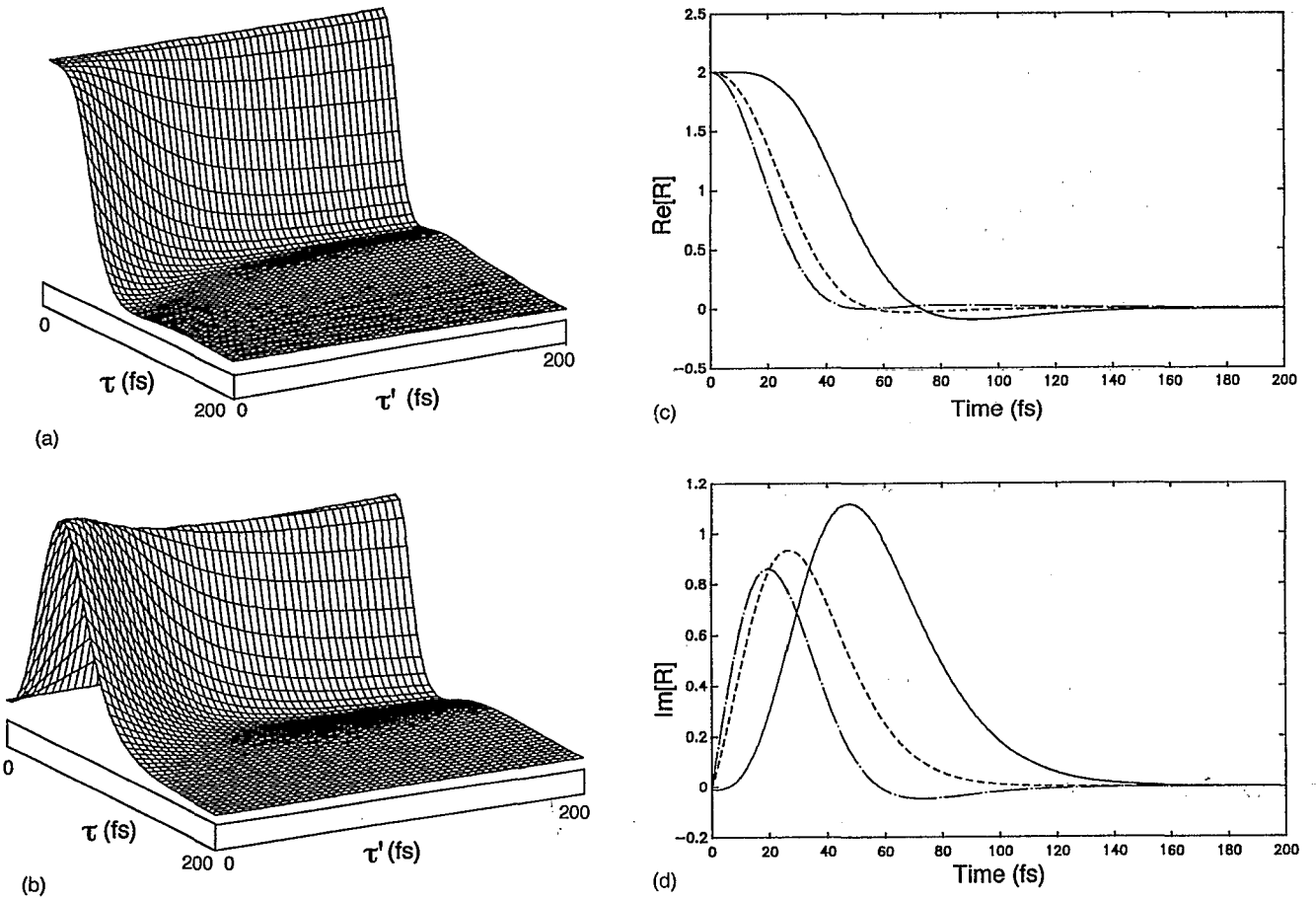

FIG. 6. Heterodyne-detected stimulated photon echo signals with $\langle\Delta\omega^2\rangle=600\ \mathrm{ps}^{-1}$ and $\lambda=50\ \mathrm{ps}^{-1}$. (a) Real part of the echo-response function. (b) Imaginary part of the echo-response function. (c) Real parts of the echo-response function with respect to τ for $\tau'=0$ (solid curve), 50 fs (dashed curve), and 100 fs (dashed-dotted curve). (d) Imaginary parts of the echo-response function with the same parameters as in (c).

the excited state lifetime which is usually long on this time scale.

D. When the solvation correlation function [$S(t)$] is used for $M(t)$ with a finite Stokes shift (nonzero λ)

Up to this point we have considered model systems without spectral diffusion, i.e., $\lambda=0$. Using $S(t)$ for $M(t)$ and assuming $\lambda=50\ \mathrm{ps}^{-1}$ ($1667\ \mathrm{cm}^{-1}$), we calculate response functions including spectral diffusion. If the spectral diffusion is ignored, the imaginary part of the response function vanishes and the lineshape function $g(t)$ is purely real. For the model system with spectral diffusion, both the real and imaginary parts of $R(\tau,\tau',\tau)$ are shown in Figs. 6(a) and 6(b), respectively. Experimental measurements of both real and imaginary parts of R are only possible using the heterodyne-detected stimulated photon echo technique (see Ref. 10).

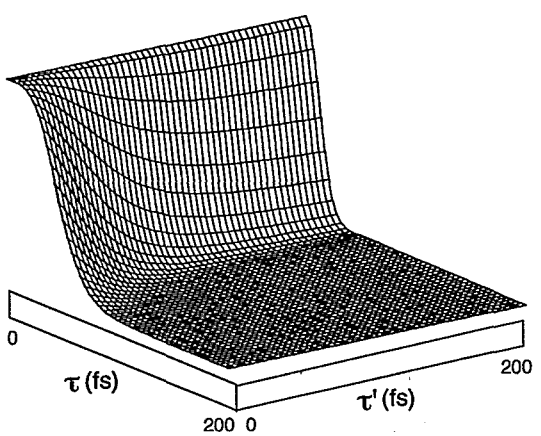

FIG. 7. Three-pulse photon echo signals (stimulated photon echo signals) with $\langle\Delta\omega^2\rangle=600\ \mathrm{ps}^{-1}$ and $\lambda=50\ \mathrm{ps}^{-1}$.

The real and imaginary parts of the response function with respect to τ' for constant values of $\tau=0$, 50, and 100 fs are shown in Figs. 6(c) and 6(d). The real part of R at $\tau'=0$ is the same as the case studied in Sec. IV C with $\lambda=0$. Therefore, the spectral diffusion process cannot be observed in a two-pulse photon echo measurement. The imaginary part of R initially increases before decaying. In Fig. 7 we show $|R(\tau,\tau',\tau)|^2$. The two-pulse echo signal is obtained at $\tau'=0$.

E. Using $M(t)=S(t)$ with various λ's and $\langle\Delta\omega^2\rangle$'s

In the preceding sections, the solvent fluctuation amplitude $\langle\Delta\omega^2\rangle$ was assumed to be $600\ \mathrm{ps}^{-2}$. In order to separately study the influences of spectral diffusion and electronic dephasing processes on the photon echo signals,

we ignore the relationship between λ and $\langle\Delta\omega^2\rangle$ mediated by the fluctuation-dissipation theorem.[9] In Fig. 8 we show echo signals with $\lambda=50$ ps^{-1} and $\langle\Delta\omega^2\rangle=600$, 400, and 200 ps^{-2}. Both real and imaginary parts of the response function for $\tau'=0$ show a very weak dependence on $\langle\Delta\omega^2\rangle$ in the initial 75 and 50 fs, respectively. By contrast, the conventional two-pulse photon echo signal shown in Fig. 8(c) is very sensitive to the magnitude of the solvent fluctuation.

A second series of calculations varied λ from 10 to 50 ps^{-1} with a constant $\langle\Delta\omega^2\rangle=600$ ps^{-2}. The results are shown in Fig. 9. As the spectral diffusion amplitude increases, the decay rate of the real part of the response function increases. Likewise, the rise time of the imaginary response function in Fig. 9(b) decreases as λ increases. On the other hand, as Fig. 9(c) shows the conventional two- or three-pulse echo signals when τ is varied do not depend on the spectral diffusion parameter. The insensitivity of the conventional echo signals to λ when measured with respect to τ arises because the real and imaginary parts are complementary and contribute the same magnitude to $|R(\tau,0,\tau)|^2$ [see Fig. 9(d)].

V. DISCUSSION

The calculations described earlier enable us to make a number of comments on the physical basis of photon echo signals in solutions. The dynamical aspects of the solvent are represented by the time-dependent behavior of the correlation function $M(t)$. The complexity of the solvation process observed in experiments[18] and molecular-dynamics (MD) simulation studies[17,22–24] shows that simple models, such as the Bloch equation, the exponential model, and the Gaussian model, provide inadequate descriptions of the dynamical content of echo signals. The dominant role of solvent inertial motion emerges clearly from the comparison of calculations using the experimental solvation correlation functions and a simple Gaussian approximation. Recently, Shemetulskis and Loring also found a major role for inertia in their molecular dynamics simulations of two-pulse echo signals.[6(b)] The small difference between the echo signal calculated using the full $S(t)$ function and the Gaussian approximation in Fig. 5 suggests that photon echo measurements preferentially detect the fastest solvent fluctuations.

The inertial behavior of the solvent molecules in solvation dynamics is well-characterized by a Gaussian decay at short times. To understand the inertial effect on the echo signal, we expand the correlation function $M(t)$ as $M(t)\cong 1-t^2/\tau_g^2+\cdots$. From Eq. (8a) the two-pulse photon echo signal is then approximated as

$$S_{\mathrm{PE}}(\tau)=4\exp\{-2\langle\Delta\omega^2\tau^4/\tau_g^2\} \tag{16}$$

for short time. In Fig. 10, we compare the aforementioned short-time expression with the two-pulse echo signal. Although the echo signals up to 30 fs are very similar, the short-time expression decays too quickly after this. The limitation of Eq. (16) is clear. The long-time decay (30–100 fs for the particular value of $\langle\Delta\omega^2\rangle=600$ ps^{-1}) in the echo signals represents the contribution from the intermediate part (100 fs–1 ps) of the solvent fluctuation correlation function.

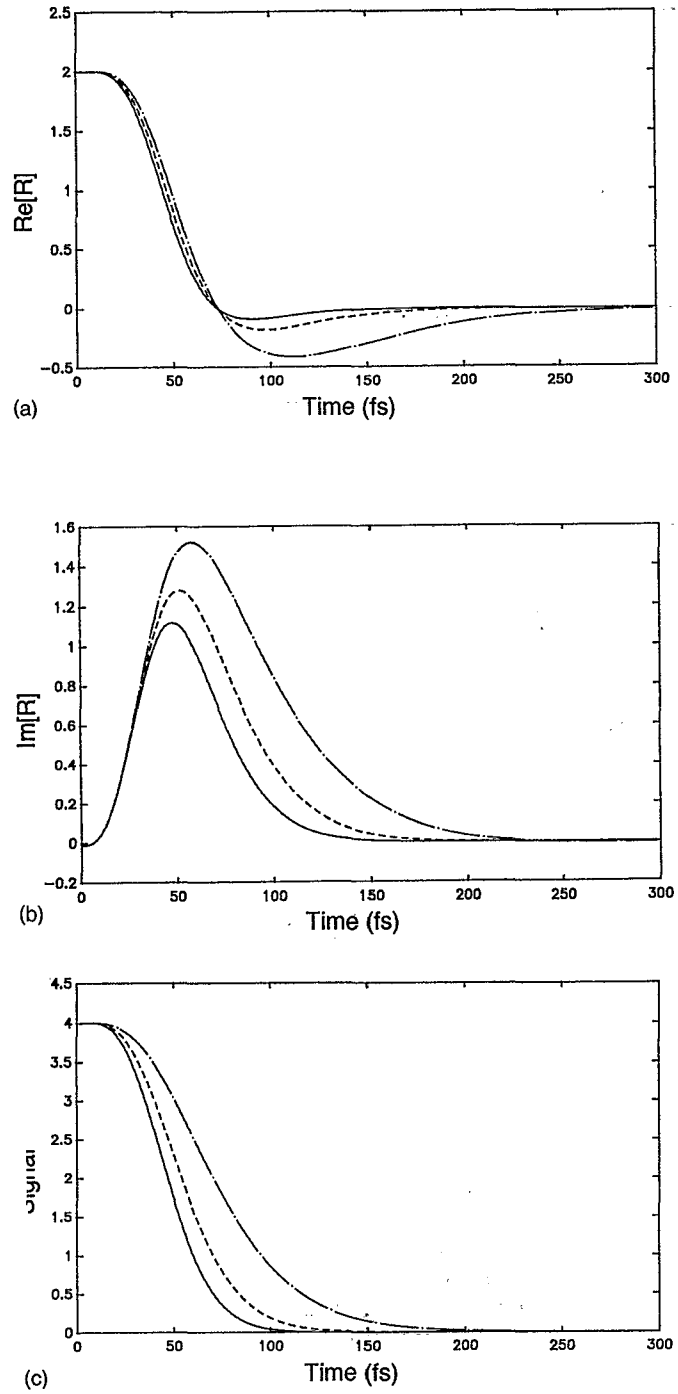

FIG. 8. (a) Real parts of the response function with respect to τ with $\lambda=50$ ps^{-1} for $\langle\Delta\omega^2\rangle=600$ (solid curve), 400 (dashed curve), and 200 ps^{-2} (dashed-dotted curve). (b) Imaginary parts of the response function with the same parameters as in (a). (c) Two-pulse photon echo signals with respect to τ with $\lambda=50$ ps^{-1} for $\langle\Delta\omega^2\rangle=600$ (solid curve), 400 (dashed curve), and 200 ps^{-2} (dashed-dotted curve).

The applicability of the Markov approximation has been discussed numerous times in the context of liquid-phase dynamics. The Markovian limit arises when the correlation function of the fluctuation decays sufficiently rapidly. More specifically, the decay constant should be much

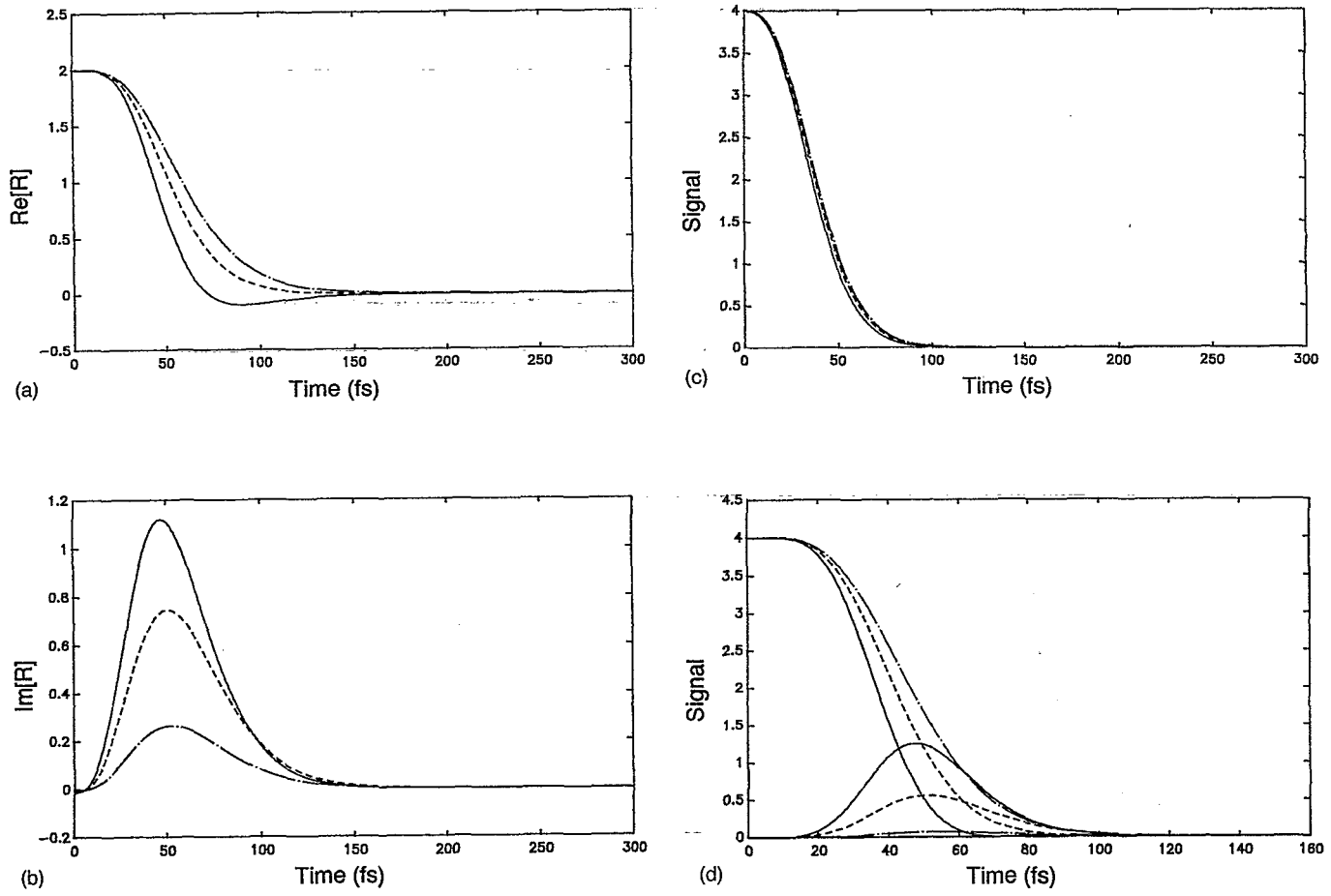

FIG. 9. (a) Real parts of the response function with respect to τ with $\langle\Delta\omega^2\rangle=600$ ps^{-2} for $\lambda=50$ (solid curve), 30 (dashed curve), and 10 ps^{-1} (dashed-dotted curve). (b) Imaginary parts of the response function with the same parameters as in (a). (c) Three-pulse photon echo signals with respect to τ and $\tau'=20$ fs. The mean-square fluctuation $\langle\Delta\omega^2\rangle$ is 600 ps^{-2} for $\lambda=50$ (solid curve), 30 (dashed curve), and 10 ps^{-1} (dashed-dotted curve). (d) The upper three curves correspond to $[\mathrm{Re}\{R(\tau,0,\tau\}]^2$ for $\lambda=50$ (solid curve), 30 (dashed curve), and 10 ps^{-1} (dashed-dotted curve), and the lower three curves correspond to $[\mathrm{Im}\{R(\tau,0,\tau\}]^2$ with the same notation and values of λ.

smaller than the inverse of the root-mean square fluctuation, i.e., $(\langle\Delta\omega^2\rangle)^{1/2}\ll\tau_c^{-1}$ in the case of the exponential model (see Sec. IV C). The physical meaning of this condition is that the width of the frequency distribution of the solvent fluctuation is much broader than $(\langle\Delta\omega^2\rangle)^{1/2}$. For example, the exponential model system can be characterized by a Lorentzian spectral density whose width is τ_c^{-1}. The width of the spectral density for the model system whose τ_c is 10 fs, is 100 ps^{-1} which is much larger than $(\langle\Delta\omega^2\rangle)^{1/2}=24$ ps^{-1}, when $\langle\Delta\omega^2\rangle=600$ ps^{-2}. Thus, the Markovian limit, also called the white noise limit, is valid only when the root mean square of the solvent fluctuation amplitude is much smaller than the spectral distribution of the solvent fluctuations. Since there is no apparent relation between the bath fluctuation amplitude and the correlation time constant, it is necessary to compare these two quantities to decide if the system is in Markovian limit.

When τ_c is 200 fs, the width of this exponential model system is 5 ps^{-1}. Clearly, this is smaller than $(\langle\Delta\omega^2\rangle)^{1/2}$. Therefore, the echo signal is now nonexponential or non-Markovian (intermediate modulation regime). Although the asymptotic limit of the echo signal should be exponen-

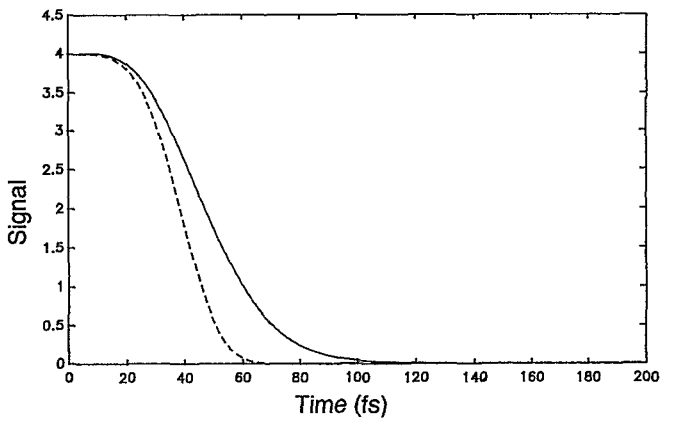

FIG. 10. The two-pulse photon echo signal calculated with the short-time expression given in Eq. (16) is shown as the dashed curve. The solid curve is identical to the two-pulse photon echo shown in Fig. 5(a).

tial if $\tau \gg \tau_c$, the echo signal intensity may well be too weak in this time region to be detected. Since the two-pulse photon echo signal is simply given by

$$S_{\mathrm{PE}}(\tau)=\exp\{-2\,\mathrm{Re}[4g(\tau)-g(2\tau)]\}, \tag{17}$$

the signal at short times can be approximated as (for this exponential model system)

$$S_{\mathrm{PE}}(\tau\cong 0)=\exp\left\{-\langle\Delta\omega^2\rangle\left[\frac{4\tau^3}{3\tau_c}-\frac{\tau^4}{\tau_c^2}+O\left(\frac{\tau^5}{\tau_c^3}\right)\right]\right\}. \tag{18}$$

The major difficulty with the exponential model is that both the inertial contribution and the slower part of the response (i.e., the bimodal character) are missing in the solvent fluctuation correlation function. The τ'-dependent signals in Fig. 4(b) show that as the fixed value of τ increases the signal is simply shifted to shorter times. Shank *et al.* observed this behavior in three-pulse photon echo measurements.[13] For fixed delay times between the first and third pulses, they observed a series of decays with the same decay pattern (see Fig. 1 in Ref. 13).

The inertial character of the solvent response is included in the Gaussian approximation to $M(t)$. In this case, the solvent dynamics are not in the Markovian limit, since the width of the spectral density of the solvent fluctuations is approximately $\tau_g^{-1}=16\ \mathrm{ps}^{-1}$, which is comparable to $(\langle\Delta\omega^2\rangle)^{1/2}=24\ \mathrm{ps}^{-1}$. Nonexponential decay in the echo signal is also apparent.

Our numerical calculations emphasized the importance of the solvent fluctuation amplitude. It would be very interesting to obtain the amplitude of the solvent fluctuation for different combinations of solvent and solute molecules. Moreover, it will be interesting to test the assumption of $M(t)=S(t)$ obtained from the time-dependent fluorescence Stokes shift or molecular-dynamics simulations. When spectral diffusion is included in the model the imaginary part of the response function becomes nonzero. This situation is likely to apply to all polar molecules in polar solvents. In this case the additional information content present in the heterodyne-detected echo signals becomes apparent, and should allow a more complete description of the dynamical aspects of the solvent system. Oscillatory behavior can be observed both in the heterodyne-detected echo signals and in the two- or three-pulse photon echo signals. The oscillation frequency is determined mostly by the magnitude of the Stokes shift λ. The τ'-dependent measurement for a fixed value of τ is governed by the spectral diffusion process as can be seen in Figs. 6(a), 6(b), and 7. As is well known, because the final interactions are coincident, the two-pulse echo signal is independent of spectral diffusion. This is also the case for stimulated photon echoes measured with respect to τ not τ'.

The spectral diffusion in the photon echo measurements during τ' occurs on either the excited or the ground potential-energy surfaces. On the other hand, the spectral diffusion during the electronic coherence states occurs neither on the excited nor on the ground potential-energy surfaces. Two approximations have been employed in simulations, that the electronic coherences propagate on either the ground or excited states[25] or on the arithmetic mean of the ground- and excited-state potential-energy surfaces.[6(b)] The heterodyne detected echo measurement allows the additional possibility of probing spectral diffusion during τ, i.e., when the system is in an electronic coherence as shown in Figs. 8 and 9. This should allow tests of the various classical approximations to this quantum mechanical system.

A fluorescence Stokes shift can be understood as an energy dissipation (depopulation) process from the solute to the bath through the solvation process, since the diagonal density matrix of the electronic excited state is being probed. The decay of the off-diagonal density-matrix elements observed in the echo measurement during an electronic coherence period (here it is during τ) contains information on the phase relaxation through depopulation and pure homogeneous dephasing. Here, we broaden the term depopulation process to include the intrinsic lifetime contribution of the excited state as well as spectral diffusion. As seen in Figs. 8 and 9, the spectral diffusion contribution during an electronic coherence is directly related to the initial decay and rise of the real and imaginary parts of the HSPE signal measured during τ, while the conventional τ-dependent echo signal is only sensitive to the pure homogeneous and lifetime contributions. In other words, the insensitivity of the conventional echo signals to the spectral diffusion during the electronic coherence state reveals that information on the spectral diffusion contribution to the electronic coherence propagation could be lost. To illustrate this, we summarize the various contributions to the echo response functions during each period as in the following.

(i) The first electronic coherence state (t_1): pure electronic dephasing process, lifetime broadening of the excited state of the chromophore, and spectral diffusion process on the quantum-mechanical mixed potential surface.

(ii) The excited and ground population states (t_2): lifetime broadening of the excited state of the chromophore for the excited population state and spectral diffusion on the excited and the ground potential surfaces, respectively. During the propagation of the excited population state, structural reorganization of the surrounding solvent system occurs.

(iii) The second electronic coherence state (t_3): pure electronic dephasing process, lifetime broadening of the excited state of the chromophore, and spectral diffusion process on the quantum mechanical mixed potential surface (during or after structural reorganization of the solvent if the propagation of the population state was on the excited potential surface). Now, the conventional echo signal [which measures the echo intensity rather than the echo field during the electronic coherence period (t_1 and t_3)] measures the pure electronic dephasing and lifetime broadening contributions without the spectral diffusion contribution which could be different from the spectral diffusion during the population state (t_2). The absence of spectral diffusion from the τ-dependent conventional three-pulse echo signal is clearly demonstrated in Fig. 9(c). On the other hand, as Fig. 9(d) shows HSPE measurements

do reveal the result of spectral diffusion during the coherence periods. This is because the HSPE signal contains the phase information of the echo field, while the conventional echo signal includes only the amplitude of the echo field.

The ability to control the period between the third and fourth pulses in the HSPE experiment (see Fig. 1) provides an opportunity to probe the time-dependent (τ_3-dependent) echo intensity after the third interaction with the external field. If the large inhomogeneous broadening limit is applicable, the echo field should be peaked at $t=\tau$ from the third pulse when the delay time between the first and second pulses is τ. To our knowledge, this is the only experimental technique that makes it possible to probe the third time period (t_3). In addition, the fluctuation amplitude $\langle\Delta\omega^2\rangle$ can be measured without any contribution from the inhomogeneity.

Many different techniques have been used to investigate liquid-state dynamics. Generally, the data have been analyzed according to phenomenological models making it difficult to compare the dynamical character of one liquid with another, or to assess the consistency and information content of the various different experiments.[26] At this point it may be appropriate to discuss Brownian oscillator models for the solvation fluctuation correlation function. The Brownian oscillator model is useful for describing the solvent dynamics with a few characteristic parameters, i.e., frequency of the oscillators and damping constants.[27] With the Markovian approximation for the friction kernel (i.e., the memory kernel is a δ function), Fried *et al.* calculated nonlinear response functions by using several Brownian oscillators to mimic the water fluctuation correlation function.[25] The disadvantage of simulating the time-dependent behavior of the solvent fluctuation with stochastic model is that potentially useful information on the solvent–solute interactions can be lost if the solvent dynamics are not described in terms of microscopic quantities, such as intermolecular potential and pair correlation functions, liquid structures, etc.

We suggest that it would be useful to describe the liquid dynamics with a characteristic spectral density which will allow connections between different experimental observations to be made in a unified way. The spectral density basically represents the distribution of the dynamical time scales in the liquid. For example, the role of low-frequency fluctuations in providing inhomogeneity on a particular time scale can be clarified and systematically investigated. Recently, an attempt along these lines was carried out by Cho *et al.*,[19] in which the short-time behavior observed in both the optical Kerr effect and time-resolved fluorescence Stokes shift measurements on acetonitrile were analyzed by a model spectral density. Buchner *et al.* have made a very similar suggestion as a result of their work on instantaneous normal modes in liquids.[28]

Many challenges exist in the implementation of this program. The projection of the spectral density onto specific observations must be addressed. In the case of acetonitrile we assumed[19] that the same spectrum is responsible for both optical Kerr effect and solvation correlation function signals. Although this worked well in this case it is unlikely to do so in general. For example, in water we might expect the librational modes to play a much stronger role in the solvation process than the Kerr response. The time scale on which inherent structures[4] persist in the liquid is also critical. For water the simulations of Ohmine *et al.*[4(b),4(c)] suggest a time scale in the tens of picoseconds, although this time may be much shorter in less structured liquids. Finally, the transition from inertial to diffusive motion must be included, although the unexpected importance of the inertial contribution to many experimental signals makes this less important than was expected for interpretation of ultrafast spectroscopic studies.

ACKNOWLEDGMENTS

This work was supported by the National Science Foundation. The authors wish to thank Professor S. Mukamel for very helpful discussions.

[1] R. A. Marcus and N. Sutin, Biochim. Biophys. Acta. **811**, 265 (1985); J. Jortner, J. Chem. Phys. **65**, 4860 (1976); M. D. Newton and N. Sutin, Annu. Rev. Phys. Chem. **35**, 437 (1984); G. L. Closs and J. R. Miller, Science **240**, 440 (1988); L. D. Zusman, Chem. Phys. **49**, 295 (1980); J. T. Hynes, J. Phys. Chem. **90**, 3701 (1986); H. Sumi and R. A. Marcus, J. Chem. Phys. **84**, 4894 (1986); I. Rips and J. Jortner, *ibid.* **87**, 6513 (1987); S. Mukamel and Y. J. Yan, Acc. Chem. Res. **22**, 301 (1989); J. Jean, R. A. Friesner, and G. R. Fleming, J. Chem. Phys. **96**, 5827 (1992).

[2] J. T. Hynes, *The Theory of Reactions in Solution*, Vol. IV of *The Theory of Chemical Reaction Dynamics*, edited by M. Baer (CRC Press, Boca Raton, FL, 1985); p. 171; P. Hänggi, P. Talkner, and M. Borkovec, Rev. Mod. Phys. **62**, 251 (1990); R. M. Whitnell and K. R. Wilson Rev. Comp. Chem. Vol. IV, edited by K. B. Lipowitz and D. B. Boyd (VCH, New York, 1993); p. 67.

[3] J. B. Birks, *Photophysics of Aromatic Molecules* (Wiley, New York, 1970); S. Mukamel, Annu. Rev. Phys. Chem. **41**, 647 (1990); J. T. Fourkas and M. D. Fayer, Acc. Chem. Res. **25**, 227 (1992); K. A. Nelson and E. P. Ippen, Adv. Chem. Phys. **75**, 1 (1989).

[4] (a) F. H. Stillinger and T. A. Weber, Phys. Rev. **25**, 978 (1982); **28**, 2408 (1983); J. Phys. Chem. **87**, 2833 (1983); Science **225**, 983 (1984); (b) I. Ohmine, H. Tanaka, and P. G. Wolynes, J. Chem. Phys. **89**, 5852 (1988); (c) I. Ohmine and H. Tanaka, *ibid.* **93**, 8138 (1990).

[5] R. A. Harris, R. A. Mathies, and W. T. Pollard, J. Chem. Phys. **85**, 3744 (1986).

[6] (a) N. E. Shemetulskis and R. F. Loring, J. Chem. Phys. **95**, 4756 (1990); (b) N. E. Shemetulskis and R. F. Loring, J. Chem. Phys. **97**, 1217 (1992).

[7] I. D. Abella, N. A. Kurnit, and S. R. Hartmann, Phys. Rev. A **141**, 391 (1966); T. Mossberg, A. Flushberg, R. Kachru, and S. R. Hartmann, Phys. Rev. Lett. **42**, 1665 (1979); W. H. Hesselink and D. A. Wiersma, *ibid.* **43**, 1991 (1979).

[8] Y. R. Shen, *The Principles of Nonlinear Optics* (Wiley, New York, 1984); L. Allen and J. H. Eberly, *Optical Resonance and Two-Level Atoms* (Wiley, New York, 1975).

[9] Y. J. Yan and S. Mukamel, J. Chem. Phys. **94**, 179 (1991).

[10] M. Cho, N. F. Scherer, G. R. Fleming, and S. Mukamel, J. Chem. Phys. **96**, 5618 (1992).

[11] (a) A. M. Weiner, S. De Silvestri, and E. P. Ippen, J. Opt. Soc. Am. B **2**, 654 (1985); (b) A. M. Weiner, S. De Silvestri, and E. P. Ippen, in *Ultrafast Phenomena IV*, edited by D. H. Auston and K. B. Eisenthal (Springer–Verlag, Berlin, 1984), pp. 230–232, (c) K. Duppen and D. A. Wiersma, J. Opt. Soc. Am. B **3**, 614 (1986); (d) D. A. Wiersma and K. Duppen, Science **237**, 1147 (1987).

[12] P. C. Becker, H. L. Fragnito, J.-Y. Bigot, C. Brito-Cruz, R. L. Fork, and C. V. Shank, Phys. Rev. Lett. **63**, 505 (1989).

[13] J.-Y. Bigot, M. T. Portella, R. W. Schoenlein, C. J. Bardeen, A. Migus, and C. V. Shank, Phys. Rev. Lett. **66**, 1138 (1991).

[14] E. T. J. Nibbering, D. A. Wiersma, and K. Duppen, Phys. Rev. Lett. **66**, 2464 (1991).

[15] S. Mukamel, Phys. Rev. A **28**, 3480 (1983).

[16] S. Mukamel and R. F. Loring, J. Opt. Soc. Am. B **3**, 595 (1986); S. Mukamel, Annu. Rev. Phys. Chem. **41**, 647 (1990).
[17] E. A. Carter and J. T. Hynes, J. Chem. Phys. **94**, 5961 (1991).
[18] S. J. Rosenthal, X. Xie, M. Du, and G. R. Fleming, J. Chem. Phys. **95**, 4715 (1991).
[19] M. Cho, S. J. Rosenthal, N. F. Scherer, L. D. Ziegler, and G. R. Fleming, J. Chem. Phys. **96**, 5033 (1992).
[20] W. Bosma, Y. J. Yan, and S. Mukamel, J. Chem. Phys. **93**, 3863 (1990).
[21] N. Bloembergen, E. M. Purcell, and R. V. Pound, Phys. Rev. **73**, 679 (1948); R. Kubo, Adv. Chem. Phys. **15**, 101 (1969).
[22] (a) M. Maroncelli and G. R. Fleming, J. Chem. Phys. **86**, 6221 (1987); (b) M. Maroncelli, *ibid.* **94**, 2085 (1991).
[23] K. Ando and S. Kato, J. Chem. Phys. **95**, 5966 (1991).
[24] E. Neria and A. Nitzan, J. Chem. Phys. **96**, 5433 (1992); L. Perera and M. L. Berkowitz, *ibid.* **96**, 3092 (1992).
[25] L. E. Fried, N. Bernstein, and S. Mukamel, Phys. Rev. Lett. **68**, 1842 (1992).
[26] In this context it is appropriate to point out the comparison between hole burning [C. H. Brito Cruz, R. L. Fork, W. H. Knox, and C. V. Shank, Chem. Phys. Lett. **132**, 341 (1986)] and photon echo measurements (Ref. 13) made on the same system by Shank and co-workers.
[27] For a detailed simulation of the complicated solvent dynamics, it will be necessary to introduce a time-dependent memory kernel, in which the multidimensional nature of the solvent degrees of freedom are included in the memory kernel by eliminating the bath degrees of freedom by way of the projection operator techniques. [R. Zwanzig, in *Lectures in Theoretical Physics*, edited by W. E. Brittin, B. W. Downs, and J. Downs (Interscience, New York, 1961), Vol. 3, p. 106; H. Mori, Progr. Theor. Phys. (Tokyo) **33**, 423; **34**, 399 (1965).] However, the absence of a general method to obtain the memory kernel makes this approach impractical for the analysis of spectroscopic observations.
[28] M. Buchner, B. M. Ladanyi, and R. M. Stratt, J. Chem. Phys. **97**, 8522 (1992).